③

Electrostatic Whistler Mode Conversion

at Plasma Resonance

J. E. Maggs and G. J. Morales

February 1988

DTIC
ELECTED
MAR 2 8 1988

H

CENTER FOR
PLASMA PHYSICS
AND
FUSION ENGINEERING

UNIVERSITY OF CALIFORNIA
LOS ANGELES

88 3 08 059

Electrostatic Whistler Mode Conversion

at Plasma Resonance

J. E. Maggs and G. J. Morales

DTIC
ELECTE
MAR 2 8 1988

University of California

Department of Physics

Los Angeles, CA 90024-1547

ELECTROSTATIC WHISTLER MODE CONVERSION
AT PLASMA RESONANCE

J.E. Maggs and G.J. Morales
Physics Department,
University of California at Los Angeles,
Los Angeles, CA 90024

ABSTRACT

The mode conversion of an electrostatic whistler wave into a
Bohm-Gross mode at plasma resonance is analyzed for a magnetized plasma
with a longitudinal density gradient (i.e., $\nabla n_0 \times \vec{B} = 0$). It is found
that a whistler incident upon plasma resonance from inside the plasma
converts, without producing a reflected wave, into a short wavelength
Bohm-Gross mode that carries energy down the density gradient away
from resonance. The detailed structure of the electric field near the
resonance is found analytically. It is shown that the production of
the Bohm-Gross wave by mode conversion can be described by a model of
plasma resonance driven by a $k=0$ electric field (i.e., the capacitor
plate model). The relation between the driver amplitude and the
amplitude of the incident whistler is derived.

I. <u>Introduction:</u>

This paper analyzes the process of mode conversion of a long wavelength electrostatic whistler wave into a short wavelength Bohm-Gross mode. The whistler with frequency ω, less than the electron gyrofrequency, Ω (i.e., $\omega < \Omega$), propagates from inside the plasma in the direction of decreasing density to the plasma resonance point, $\omega_{pe} = \omega$, (ω_{pe} is the electron plasma frequency) where mode conversion occurs.

The electrostatic whistler waves considered here satisfy the dispersion relation $\varepsilon_{\parallel} k_{\parallel}^2/k^2 + \varepsilon_{\perp} k_{\perp}^2/k^2 = 0$, where in the cold plasma limit $\varepsilon_{\parallel} = 1 - \omega_{pe}^2/\omega^2$ and $\varepsilon_{\perp} = 1 - \omega_{pe}^2/(\omega^2-\Omega^2)$. In a magnetized plasma in which the density varies only along the magnetic field direction, z, as illustrated in Fig. 1, the WKB wave number component along the magnetic field, $k_{\parallel} = k_{\perp}(-\varepsilon_{\perp}/\varepsilon_{\parallel})^{1/2}$, is a function of position. As the whistler wave propagates towards lower densities so that ω_{pe} approaches ω, $\varepsilon_{\parallel}$ approaches zero and the parallel wave number becomes large. The inclusion of finite temperature effects in the parallel dielectric component, $\varepsilon_{\parallel}$, then allows the long wavelength whistler wave to couple to the short wavelength Bohm-Gross mode near plasma resonance. The whistler wave propagating to plasma resonance then mode converts into a short wavelength thermal mode that propagates away from resonance towards decreasing density.

This particular mode conversion process is of general interest because it represents a channel for converting wave energy into fast electrons. The auroral ionosphere which is characterized by non-thermal levels of whistler waves and field-aligned electron distributions is a natural plasma in which this process is likely to occur. In the auroral ionosphere the density gradient in the background plasma is aligned nearly along the magnetic field so that a model plasma with a field aligned

density gradient is appropriate for describing this environment. Whistler mode conversion may occur naturally in the auroral ionosphere or be stimulated artifically by launching waves from polar orbiting spacecraft.

The main purpose of this study is to determine analytically the detailed structure of the electric fields involved in the mode conversion process. This knowledge can then be used in later computations to determine the changes in the electron distribution produced by acceleration from the mode converted whistler wave.

In section II the equation governing the structure of the electric potential is derived and an integral representation of the general solutions is obtained. Asymptotic and series expressions for the short wavelength solutions are obtained in section III while the properties of the long wavelength solutions are examined in section IV. The mode conversion process is treated in section V and the structure of the mode converted electric field is determined in section VI. Conclusions are presented in section VII.

II. Governing Equation:

The equation determining the structure of the electric potential in the plasma is

$$\underline{\nabla} \cdot \underline{\underline{\varepsilon}} \cdot \underline{\nabla} \, \Phi = 0, \tag{1}$$

where Φ is the electric potential and $\underline{\underline{\varepsilon}}$ the plasma dielectric tensor operator. For the model plasma described here, the electric potential amplitude, ϕ, varies only along the z-direction and Φ can be written in the form

$$\Phi(x,z,t) = \phi(z)\exp\left(i(k_\perp x - \omega t)\right). \tag{2}$$

Furthermore the plasma dielectric tensor components depend only upon z

and in the cold plasma limit are: $\varepsilon_{xz} = \varepsilon_{zx} = \varepsilon_{yz} = \varepsilon_{zy} = 0$, $\varepsilon_{xx} = \varepsilon_{yy} = \varepsilon_{\perp}$, $\varepsilon_{xy} = -i(\Omega/\omega)(\varepsilon_{\perp}-1) = -\varepsilon_{yx}$, and $\varepsilon_{zz} = \varepsilon_{\parallel}$.

A plasma with a nonzero temperature supports modes which propagate both along (Bohm-Gross modes) and perpendicular (Bernstein modes) to the magnetic field. The Bohm-Gross modes arise from thermal corrections to the parallel component of the cold plasma dielectric, $\varepsilon_{\parallel}$, while the Bernstein modes arise from thermal corrections to the perpendicular component, $\varepsilon_{\perp}$. However, since we are considering whistler waves which necessarily have $\omega < \Omega$ we need not consider coupling to Bernstein modes. In addition, we consider the case in which the electron gyroradius $(v_{\perp}/\Omega)$ is much smaller than the perpendicular wave length so that thermal corrections to the perpendicular dielectric component are negligible.

The lowest order thermal corrections to the parallel component of the plasma dielectric cause it to become a differential operator,

$$\varepsilon_{\parallel} = 1 - \frac{\omega_p^2}{\omega^2} + \gamma\frac{\bar{v}^2}{\omega^2}\frac{d^2}{dz^2} \quad , \qquad (3)$$

where $\bar{v}$ is the thermal velocity, $\sqrt{(2T/m)}$, and ω_p is the electron plasma frequency which, here, is a function of z. The factor γ has the value three since the electron motion is essentially one-dimensional. The parallel wave number usually appearing in the Bohm-Gross dispersion relation has been replaced by the operator, $-i\,d/dz$, because the plasma is nonuniform in the z-direction.

Since the mode conversion process occurs in the immediate vicinity of plasma resonance we make the approximation that the density varies linearly along the magnetic field with scale length, L, the density scale length at plasma resonance. The plasma frequency can then be written as

$$\omega_{pe}^2/\omega^2 = 1 - z/L = 1 - \hat{z} , \qquad (4)$$

where $\hat{z}$ is the dimensionless position variable, z/L. Since the number density in the plasma is always positive, $\hat{z}$ must be restricted to the regime less than unity in order to model a physical plasma. Using (4) the perpendicular and parallel plasma dielectric components become,

$$\epsilon_\perp = (\hat{z} - Y^2)/(1-Y^2) \; ; \; \epsilon_{||} = \hat{z} + \gamma \; \epsilon^2 \frac{d^2}{d\hat{z}^2} , \qquad (5)$$

where $Y = \Omega/\omega$ and $\epsilon^2 = \gamma \bar{v}^2/(\omega^2 L^2)$. Using (2) and (5) in (1) then results in,

$$\epsilon^2 \; \phi^{(4)} + \hat{z}\phi^{(2)} + \alpha\phi^{(1)} + (\hat{z}\beta_2^2 - \beta_1)\phi = 0 , \qquad (6)$$

which determines the spatial structure of the electric potential. Equation (6) has the same form as the equation analyzed by Maggs, et. al. (1984) except for the sign of the term proportional to ϕ. The sign difference arises because here $\omega < \Omega$, while the earlier work treated the case $\omega > \Omega$. In (6) the parameters β_1 and β_2 depend upon the perpendicular wave number,

$$\beta_2^2 = \frac{k_\perp^2 L^2}{Y^2 - 1} , \qquad \beta_1 = Y^2 \; \beta_2^2 , \qquad (7)$$

and the notation $\phi^{(j)}$ denotes the jth derivative with respect to $\hat{z}$.

The parameters β_1 and β_2^2 are real and positive since the electrostatic mode is in the whistler band and $\omega < \Omega$ so that $Y > 1$. The parameter α has the value unity for a plasma, but we consider general values of α in the mathematical analysis of Eq. (6) because this procedure is necessary to obtain the structure of the electric field in the vicinity of plasma resonance, as pointed out by Rabenstein (1958) in his classic paper on mode conversion. The parameter $\epsilon^2 = \gamma \bar{v}^2/(\omega^2 L^2)$ is the square of

the ratio of the Debye length at plasma resonance (i.e., $\omega = \omega_{pe}$, or $\mathfrak{z} = 0$)
to the density scale length, and is here taken to be a small parameter.

If ε^2 is set equal to zero a second order differential equation,
referred to as the reduced equation, is obtained from (6). The reduced
equation determines the potential structure in the cold plasma limit.
Transforming the independent variable of the reduced equation to $\xi = 2i\beta_2\mathfrak{z}$
and substituting the function $\phi = u \exp(-\xi/2)$ results in

$$\xi u^{(2)} + (\alpha - \xi)u^{(1)} - (\alpha/2 - i\beta_0)u = 0 , \qquad (8)$$

where $\beta_0 = \beta_1/(2\beta_2)$. Equation (8) has the form of Kummer's differential
equation, and linearly independent solutions can be written as combinations
of the Kummer functions $M(a_-,\alpha;i\xi)$ and $U(a_-,\alpha;i\xi)$, where $a_- = \alpha/2 - i\beta_0$
(Slater, 1970).

In addition to the two independent solutions to the reduced equation,
another pair of basic solutions exist which depend upon ε^2 being finite
(i.e., $\varepsilon^2 \neq 0$). This solution pair is related to the Bohm-Gross modes and
thus has relatively short wave length in comparison with the solutions of
the reduced equation. The equation describing the pure thermal modes can
be obtained from (6) by setting β_2 (and hence β_1) equal to zero. Doing
this, changing the independent variable to $\eta = \varepsilon^{-2/3}\mathfrak{z}$, and writing $u(\eta)$
instead of $\phi(\mathfrak{z})$ gives, after integration,

$$u^{(3)} + \eta u^{(1)} + (\alpha - 1)u = \text{constant}. \qquad (9)$$

For the case $\alpha = 1$, Eq. (9) becomes the inhomogeneous (i.e., driven)
Airy equation for $u^{(1)}$, which is proportional to the electric field.
The short wave length solutions are thus related to Airy functions
and the integrals of Airy functions.

Since the coefficients of the derivatives in (6) are all constant or
linear functions of the independent variable $\mathfrak{z}$, general solutions can be

obtained in integral form by using the Laplace transform technique
(Coddington and Levinson, 1955). The solutions then have the form,

$$S(\tilde{z}) = \int_C ds \ \frac{e^{-s\tilde{z}}}{P(s)} \exp\left(-\int^s \frac{Q(t)}{P(t)} \ dt\right) , \tag{10}$$

where $P(s)$ and $Q(s)$ are polynomials obtained from (6) by replacing $\phi^{(n)}$
by $(-s)^n$ to obtain an expression of the form, $P(s)\tilde{z} + Q(s)$. Using this
procedure we find that $P(s) = s^2 + \beta_2^2$ and $Q(s) = \epsilon^2 s^4 - \alpha s - \beta_1$. The
contours denoted by C in (10) are chosen so that the bilinear concomitant,

$$e^{-s\tilde{z}} \exp\left(-\int^s \frac{Q(t)}{P(t)} \ dt\right) , \tag{11}$$

which is essentially the boundary term obtained after an integration by
parts, is zero at the end points of the contour. For the problem under
consideration the solutions have the form

$$S(\tilde{z}) = \int_C (s + i\beta_2)^{\alpha_+}(s - i\beta_2)^{\alpha_-} \exp\left(-(\epsilon^2 s^3/3 + s\tilde{z})\right) ds, \tag{12}$$

where,

$$\tilde{z} = z + i\epsilon^2\beta_2^2 , \tag{13.a}$$

$$\alpha_+ = \alpha/2 - 1 + i\beta \ ; \ \alpha_- = \alpha/2 - 1 - i\beta , \tag{13.b}$$

$$\beta = \beta_0 + i(\epsilon^2\beta_2^3)/2 \ ; \ \beta_0 = \beta_1/(2\beta_2), \tag{13.c}$$

The contours in the integral representation (12) must be chosen so that
the condition

$$(s - i\beta_2)^{\alpha/2 - i\beta}(s + i\beta)^{\alpha/2 + i\beta} \exp\left(-(\epsilon^2 s^3/3 + s\tilde{z})\right) = 0 , \tag{14}$$

is satisfied at the end points.

Since α_+ and α_- are not integers, the points $s = i\beta_2$ and $s = -i\beta_2$ in the complex s-plane are branch points. Therefore, to obtain analytic solutions using the integral representation it is necessary to cut the integration plane with branch lines. Since, in general, $\alpha_+ \neq \alpha_-$ the two branch points can not be connected by a single branch cut. Thus the integration plane is cut with two branch lines extending from the branch points to infinity parallel to the real axis as shown in Fig. 2. In the cut plane the term $(s-i\beta_2)^{\alpha_-}$ is single valued for $2m\pi < \theta_- < 2\pi + 2m\pi$, where θ_- denotes the argument of $s-i\beta_2$ and m is integer. The term $(s+i\beta_2)^{\alpha_+}$ is single valued for $2n\pi - \pi < \theta_+ < \pi + 2n\pi$, where θ_+ denotes the argument of $s+i\beta_2$ and n is integer.

Equation (14) can be satisfied by contours that end at the points $s = i\beta_2$ or $s = -i\beta_2$, provided that $Re(\alpha/2 \pm i\beta) > 0$, or by contours that proceed to infinity along rays such that $\exp(-\varepsilon^2 s^3/3)$ vanishes. It is convenient to define two basic classes of solutions with members denoted by A_j and B_j . The solutions A_j are obtained from the integral representation (12) by using contours that begin and end at infinity. The solutions B_j are obtained by using contours with at least one end point at $s = -i\beta_2$. Some of these contours are illustrated in Fig. 2. The solutions B_2, B_3, and B_0 are closely related to the solutions of the reduced equation given in (8). Asymptotically B_2 and B_3 represent long wavelength propagating waves. The solution A_1 is related to the $\varepsilon^2 \neq 0$ class of solutions which satisfy Eq. (9). Asymptotically A_1 represents a short wavelength propagating wave.

III. ₃hort Wave Length Solutions:

In this section we investigate the behavior of the solutions that asymptotically correspond to the short wavelength solutions of Eq. (9). We evaluate the leading term of the asymptotic series for the solutions A_j which is useful for determining their behavior at large $\tilde{z}$. We then obtain a series representation for A_j which can be used to evaluate these solutions for small $\tilde{z}$. The asymptotic expression is needed to identify the thermal mode produced in the mode conversion process while the series expansion is needed to evaluate the electric field structure near the origin (i.e., plasma resonance).

The contours describing the solutions A_j have both end points at infinity. An example of the contour for the solution labeled A_1 is shown in Fig. 2. In order for the condition (14) to be satisfied at large $|s|$, the term $\varepsilon^2 s^3/3$ must have a positive real part, i.e.

$$2\pi(2-j)/3 - \pi/6 < \arg(s) < \pi/6 + 2\pi(2-j)/3 . \tag{15}$$

The integer j in (15) labels the open sector in the s-plane of angular width $\pi/3$ centered about the angle $2\pi/3$ for $j=1$, 0 for $j=2$, and $-2\pi/3$ for $j=3$. The contour for the function A_j has its end points at infinity in the two sectors other than sector j. For example, the contour for the function A_1 proceeds to infinity in the sectors labeled by $j = 2$ and 3.

In order to study the properties of the functions A_j it is convenient to make the transformation of variables

$$\sigma = \varepsilon^{2/3} s \quad ; \quad \eta = \varepsilon^{-2/3} \tilde{z} \quad ; \quad \sigma_0 = i\varepsilon^{2/3}\beta_2 . \tag{16}$$

With this transformation, the integral representation (12) has the form

$$A_j(\eta) = \varepsilon^{-2(\alpha-1)/3} \int_{C(A_j)} (\sigma-\sigma_0)^{\alpha_-} (\sigma+\sigma_0)^{\alpha_+} \exp\left(-(\sigma^3/3 + \sigma\eta) \right) d\sigma , \tag{17}$$

where $C(A_j)$ is the image of the contour for A_j under the transformation (16).

We first investigate the asymptotic properties of the functions $A_j(\eta)$ by assuming that ϵ^2 is small and the magnitude of $\hat{z}$ is large, specifically, $|\hat{z}| \gg \epsilon^2 \beta_2^2$. The saddle point method of integration can be used to evaluate (17) under these asumptions. Defining $f(\sigma) = \sigma^3/3 + \sigma\eta$, the saddle points are determined by the condition $f'(\sigma) = 0$. Thus the integrand of (17) has two saddle points at $\sigma_s = \pm i\eta^{1/2}$. The condition of large $|\hat{z}|$ insures that $\sigma_s \gg \sigma_0$, i.e., the saddle points are far removed from the singularities in the integrand of (17). Demanding that a saddle point lie between the Stokes lines (which are located at $\arg(s) = 0$, $2\pi/3$, and $4\pi/3$) places the following restrictions on the argument ranges of the functions A_j,

$$2\pi(2-j)/3 + 2\pi/3 < \arg(\sigma_s) < 4\pi/3 + 2\pi(2-j)/3 . \qquad (18)$$

For the saddle point $\sigma = i\eta^{1/2}$ (18) gives the argument ranges

$$4\pi(2-j)/3 + \pi/3 < \theta < 5\pi/3 + 4\pi(2-j)/3 , \qquad (19.a)$$

while the saddle point $\sigma = -i\eta^{1/2}$ gives the argument ranges

$$4\pi(2-j)/3 - 5\pi/3 < \theta < -\pi/3 + 4\pi(2-j)/3 , \qquad (19.b)$$

where $\theta = \arg(\hat{z})$. The argument ranges for the two values of the saddle point are illustrated in Fig. 3.

The direction of the path of steepest descents through the saddle point is obtained by assuming $f(\sigma)$ has the form, $x^2 = f''(\sigma_s)(\sigma-\sigma_s)^2/2$, where x^2 is real and positive (i.e., has argument zero). The sign of the leading term in the saddle point method of integration is determined by choosing the sign of $x = \pm(\sigma-\sigma_0)(f''(\sigma_s)^{1/2})$ such that x is positive along the direction of the contour of integration. Thus, if the contour of

integration passes through the saddle point in the same (opposite) direction as the path of steepest descents the plus (minus) sign is chosen. Since $f''(\sigma_s)/2 = \sigma_s$, the positive direction of the path of steepest descents has $\arg(\sigma-\sigma_s) = -\arg\left[(i\eta^{1/2})^{1/2}\right]/2$ for the saddle point $\sigma_s = i\eta^{1/2}$ and $\arg(\sigma-\sigma_s) = -\arg\left[(-i\eta^{1/2})^{1/2}\right]/2$ for $\sigma_s = -i\eta^{1/2}$. The leading term in the asymptotic expression for $A_j(\eta)$ then gives, for the saddle point $\sigma_s = i\eta^{1/2}$

$$A_j(\eta) = (-)^j \ p_j \ \sqrt{\pi} \ (i\eta^{1/2})^{\alpha-5/2} \ \varepsilon^{-2(\alpha-1)/3} \ e^{-i\varsigma} , \qquad (20.a)$$

where $p_2 = p_3 = 1$, and $p_1 = e^{-i2\pi\alpha_+}$. The factor p_j in (20) arises because the saddle point for the solution A_1 lies in the Riemann sheet where the argument of the term $(\sigma-\sigma_0)^{\alpha_+}$ is 2π larger than in the principal sheet. For the saddle point $\sigma_s = -i\eta^{1/2}$

$$A_j(\eta) = (-)^{j+1} \ p_j \ \sqrt{\pi} \ (-i\eta^{1/2})^{\alpha-5/2} \ \varepsilon^{-2(\alpha-1)/3} \ e^{i\varsigma}. \qquad (20.b)$$

In (20.a) and (20.b) the variable ς is defined as $\varsigma = 2\eta^{3/2}/3$.

The asymptotic behavior of A_j as given by (20.a) and (20.b) contains the exponential term, $\exp(\pm i\varsigma)$, where $\varsigma = \frac{2}{3} \varepsilon^{-1}\hat{z}^{3/2}$. When ς is imaginary, the argument of the exponential term (i.e., $\pm i\varsigma$) is purely real and A_j is either spatially growing or decaying. For example, with $\arg(\hat{z})=\pi/3$, $\varsigma = i\frac{2}{3} \varepsilon^{-1}|\hat{z}|^{3/2}$ and , as illustrated in Fig. 3, A_2, which is asymptotically proportional to $\exp(-i\varsigma)$ as given by (20.a), represents a spatially growing function while (20.b) indicates A_1 represents a spatially decaying function.

When the variable ς is real the exponential term in (20.a,b) is oscillatory and A_j represents a propagating wave. The assumed temporal dependence $\exp(-i\omega t)$ determines whether the phase velocity of the wave is positive or negative. For example, with $\arg \hat{z} = 0$, ς is real and positive and, from (19.a) and (20.a), we see that A_3 is defined for $\arg \hat{z} = 0$ and

varies as $\exp(-i\zeta)$, while (19.b) and (20.b) indicate A_1 is defined for this argument value but varies as $\exp(i\zeta)$. The phase of A_1 then varies as $(\zeta-\omega t)$ so that A_1 asymptotically represents a positive phase velocity wave (i.e., a wave propagating left to right) for arg η = 0. Similarly A_3 , for arg η = 0, represents a right to left propagating, or negative phase velocity, wave. The asymptotic behavior of A_j at various values of the argument of η is indicated in Fig. 3.

The solutions A_j can be evaluated for small values of the independent variable η (i.e., near plasma resonance) by deriving a series expression from the integral representation (17). This can be accomplished by expanding the term $(\sigma-\sigma_0)^{\alpha_-}(\sigma+\sigma_0)^{\alpha_+}$ in the integrand of (17) in a series in σ_0/σ and integrating term by term. Carrying out this procedure (the details of the calculation are given in Appendix I) gives the following series representation of A_j , valid in the finite η-plane,

$$A_j(\eta) = \varepsilon^{-2(\alpha-1)/3} p_j \sum_k \sum_m c_m \sigma_0{}^m \frac{(-)^k}{k!} I_j(\alpha-m,k) \eta^k, \qquad (21)$$

where

$$I_j(\alpha-m,k) = 2\pi i \exp\left[\pi i(1-\rho)(7-2j)\right] / \left(3^\rho \Gamma(\rho)\right) , \qquad (22)$$

and $\rho = (4-\alpha-m-k)/3$. The phase factors p_j are the same as given previously for the asymptotic expressions (20.a,b). The restricted argument ranges given in (19.a,b) that apply to the asymptotic expressions (20.a,b) do not apply to the series expression (21) which is valid for all values of $\arg(\eta)$. Since $\sigma_0 = \varepsilon^{2/3}\beta_2$, it can be assumed, for a plasma with a gentle density gradient, to be small because $\varepsilon^2 \ll 1$. With σ_0 small, A_j can be approximated from (21) by using only the m = 0 term.

IV. Long Wave Length Solutions:

In this section we obtain approximate expressions for the solutions B_j and B_0 in terms of the well known Kummer functions M and U (Slater, 1970). The leading term of these approximations is related to the cold plasma electrostatic whistler. The expressions obtained here are used to identify the solutions that asymptotically represent whistler waves in the mode conversion solution given in Sec. V.

The contours for the solutions B_j and B_0 have at least one end point at the branch point located at $s = -i\beta_2$. To obtain an expression for B_j and B_0 in terms of familiar functions it is useful to express the integrand of (12) as a Taylor series in ϵ^2,

$$B_j(\epsilon^2) = B_j(0) + \epsilon^2 \, \partial_{\epsilon^2} B_j(0) + \ldots , \qquad (23)$$

where $B_j(0)$ is obtained by setting $\epsilon^2 = 0$ in (12),

$$B_j(0) = \int_{C(B_j)} (s + i\beta_2)^{a_+}(s - i\beta_2)^{a_-} \exp(-s\hat{s}) \, ds , \qquad (24)$$

where $a_\pm$ is $\alpha_\pm$ evaluated at $\epsilon^2 = 0$, namely

$$a_\pm = \alpha/2 \pm i\beta_0 - 1 . \qquad (25)$$

In (23) and (24) j can have the values 0, 1, 2, or 3. Since $B_j(0)$ is obtained by setting $\epsilon^2 = 0$ it is clearly a solution of the reduced equation (i.e., (6) with $\epsilon^2 = 0$). The ϵ^2 expansion given in (23) thus represents successive thermal corrections to the cold plasma whistler mode.

The solution B_0 is obtained from the contour which starts at $s = -i\beta_2$, circles the point $s = i\beta_2$ in the counter-clockwise direction and returns to the point $s = -i\beta_2$, as shown in Fig. 2. Changing the variable of

integration in (24) to s — $i\beta_2 p$ gives

$$B_0(0) = (i\beta_2)^{\alpha-1} \int_{-1}^{(1+)} dp \ (p-1)^{a-} \ (p+1)^{a+} \exp(-ip\beta_2 \hat{z}). \qquad (26)$$

In (26) the limits of integration with the notation (1+) denotes that the contour starts at p — -1, circles the point p — 1 in the counter-clockwise direction, and returns to the starting point p = -1. Since the integral representation for the Kummer function $M(b,c;x)$ for $Re(b) > 0$ is (Erdélyi, 1953),

$$M(b,c;x) = \frac{\Gamma(c)\Gamma(b-c+1)}{2\pi i \Gamma(b)} \int_0^{(1+)} e^{xt} \ t^{b-1} \ (t-1)^{c-b-1} \ dt \ , \qquad (27)$$

B_0 can be obtained in terms of $M(a,b;x)$ by changing the variable of integration in (26) to t — (p+1)/2, giving

$$B_0(0) = (2i\beta_2)^{\alpha-1} \ e^{i\beta_2 \hat{z}} \int_0^{(1+)} (t-1)^{a-} \ t^{a+} \exp(-i2\beta_2 \hat{z} t) \ dt. \qquad (28)$$

Choosing b — $a_+ + 1$ — $\alpha/2 + i\beta_0$ — α - a and c — α in (27) then gives,

$$B_0(0) = (2i\beta_2)^{\alpha-1} \ e^{i\beta_2 \hat{z}} \ \frac{2\pi i \ \Gamma(\alpha-a)}{\Gamma(\alpha)\Gamma(1-a)} \ M(\alpha-a,\alpha;-2i\beta_2 \hat{z}). \qquad (29)$$

where a — $\alpha/2 - i\beta_0$ — a_- + 1. The expression (29) is valid for all values of $\arg(\hat{z})$. The higher order corrections to B_0 in the expansion (23) can be shown to depend upon M and its derivatives with respect to β_0 (Maggs, et.al., 1984), but we do not attempt this here.

The contour for the solution $B_j(0)$ extends from s — $-i\beta_2$ to infinity in the sector labeled 'j' in Figure 1, passing above the point s — $i\beta_2$. At large |s| the integrand in (24) varies as $s^{\alpha-2} \ e^{-s\hat{z}}$. In order for the integrand to be bounded along the contour for $\alpha \geq 1$, it is necessary to

require that $\dot{z}$ be nonzero, i.e. $|\dot{z}| \geq |\dot{z}_0| > 0$ where $\dot{z}_0$ is arbitrary but small and non zero. Thus for the solutions B_j ($j = 1,2,3$) the expansion (23) is valid only for nonzero values of $\dot{z}$. This feature is evident in the Kummer function $U(b,c;x)$ which is singular at the origin for $Re(c) \geq 1$. In addition to the requirement $|\dot{z}| \geq |\dot{z}_0|$, the integrand in (24) is bounded only when $Re(s\dot{z}) > 0$, i.e.,

$$-\pi/2 < \arg(s\dot{z}) < \pi/2 \ . \tag{30}$$

The requirement (30) combined with (15) gives the argument ranges over which the functions $B_j(0)$ are defined by the integral representation (24),

$$2\pi(j-2)/3 - 2\pi/3 < \arg(\dot{z}) < 2\pi/3 + 2\pi(j-2)/3 \ . \tag{31}$$

The argument ranges given by (31) are compared to those for the functions A_j as defined by (19.a,b) in Figure 4. Using the transformation

$$s = 2i\beta_2(t+1/2) \ , \tag{32}$$

in (24) results in

$$B_j(0) = (2i\beta_2)^{\alpha-1} \ e^{-i\beta_2\dot{z}} \int_{-1}^{\infty e^{i\theta}} t^{a-} \ (t+1)^{a+} \exp(-2i\beta_2\dot{z}t) \ dt \ , \tag{33}$$

where the contour in (33) extends to infinity along a ray with $\arg(t) = \theta$.

The integral representation of the Kummer function $U(b,c;x)$ is (Erdélyi, 1953)

$$U(b,c;x) = \frac{\Gamma(1-b)}{2\pi i} \ e^{-i\pi b} \int_{\infty e^{i\theta}}^{(0+)} t^{b-1} \ (1+t)^{c-b-1} \exp(-xt) \ dt. \tag{34}$$

In (34) the contour starts at infinity with $\arg(t) = \theta$, circles the origin in the counter-clockwise direction and returns to infinity with $\arg(t) = \theta + 2\pi$. The integral in (34) can be divided into three separate integrals,

$$\int_{\infty e^{i\theta}}^{(0+)} \quad - \int_{\infty e^{i\theta}}^{-1} \quad + \int_{-1}^{(0+)} \quad + \int_{-1}^{\infty e^{i\theta + 2\pi}}$$

(35)

$$= I_1 \quad + \quad I_2 \quad + \quad I_3 \ .$$

The integral I_3 on the right hand side of (35) is like I_1 except for the direction along the contour and the argument of the variable of integration. The argument of the variable of integration in I_3 is 2π larger than in I_1 so that the term t^{b-1} in I_3 is $\exp(i2\pi p)$ times the same term in I_1 . Since the argument difference of 2π does not alter the other terms in the integrand of (34), I_3 is simply $-\exp(i2\pi p)$ times I_1 . The integral I_2 in (35) can be related to $e^{i\beta_2 \tilde{z}} M(\alpha - a, \alpha; -2i\beta_2 \tilde{z})$ by changing the variable of integration from t to $\overline{t} = t+1$. Applying (35) to (33) and using (34) then gives

$$B_j(0) = (2i\beta_2)^{\alpha - 1} \frac{\pi \ e^{-i\beta_2 \tilde{z}}}{\sin(\pi a)\Gamma(1-a)} \left\{ U(a,\alpha;2i\beta_2 \tilde{z}) \right.$$
$$\left. - \frac{e^{-i\pi a} \Gamma(\alpha - a) M(a,\alpha;2i\beta_2 \tilde{z})}{\Gamma(\alpha)} \right\}$$

(36)

where $a = \alpha/2 - i\beta_0$. Even though the subscript j does not appear explicitly on the right hand side of (36) it is present implicitly because of the argument range restrictions given by (31). Since $U(a,\alpha;2i\beta_2 \tilde{z})$ is a multivalued function the asymptotic form for B_j , as obtained from (36), depends upon the value of $\arg(\tilde{z})$ and thus on the value of j.

Equation (36) can be used to obtain asymptotic expressions for B_j that can be related directly to whistler waves in the cold plasma limit when the physical value unity is used for the parameter α (i.e. $\alpha=1$). For example, defining $w = 2i\beta_2 \tilde{z}$ and taking $\arg(\tilde{z}) = 0$ gives $\arg(w) = \pi/2$ and for this argument value the asymptotic values of $U(a,1;w)$ and $M(a,1;w)$ are

$$U(a,1;w) \sim w^{-a} , \tag{37.a}$$

$$M(a,1;w) \sim \frac{w^{-a} e^{i\pi a}}{\Gamma(1-a)} + \frac{w^{a-1} e^{w}}{\Gamma(a)} . \tag{37.b}$$

From (31) and Figure 4 we see that the argument range of B_2 contains arg $\tilde{z}$ = 0 so that using (37.a,b) in (36) gives

$$B_2(0) \sim -\Gamma(1-a) e^{-i\pi a} w^{a-1} e^{w/2} . \tag{38}$$

With the chosen time dependence $\exp(-i\omega t)$, the phase of B_2, as given by (38), varies as $2\beta_2\tilde{z} - \omega t$ so that B_2 is a left to right traveling wave for arg $\tilde{z}$ = 0, because for $\omega < \Omega$ (i.e., electrostatic whistlers) the phase velocity and group velocity are in the same direction (forward wave).

As a further example, consider the asymptotic behavior of B_j at arg $\tilde{z}$ = π, i.e. arg w = $3\pi/2$. The asymptotic values of $U(a,1;w)$ and $M(a,1;w)$ at $\arg(w)$ = $3\pi/2$ are,

$$U(a,1;w) \sim w^{-a} - \frac{2\pi i \, e^{-i\pi a} w^{-a}}{\Gamma(a)\Gamma(1-a)} - \frac{2\pi i \, w^{a-1} e^{w}}{\Gamma(a)\Gamma(a)} , \tag{39.a}$$

$$M(a,1;w) \sim \frac{e^{-i\pi a} w^{-a}}{\Gamma(1-a)} + \frac{w^{a-1} e^{w}}{\Gamma(a)} . \tag{39.b}$$

where the principal branch of the multivalued function $U(a,1;w)$ is taken as $-\pi < \arg(w) \le \pi$. From (31) we recognize that the argument range of B_3 contains the value arg $\tilde{z}$ = π so that using (39.a,b) in (36) gives

$$B_3(0) \sim -\Gamma(1-a) w^{a-1} e^{i\pi a} e^{w/2} . \tag{40}$$

Since the argument of $\tilde{z}$ is π, the phase of B_3 varies as $\beta_2|\tilde{z}| + \omega t$. For constant phase then, $|\tilde{z}|$ decreases as t increases, and since $\tilde{z}$ is negative B_3 represents a left to right propagating wave for $\arg(\tilde{z})$ = π. The direction of propagation for B_j with α = 1 is shown for selected values of arg $\tilde{z}$ in Fig. 4.

The asymptotic expressions (38) and (40) are consistent with the WKB

form of the whistler in the cold plasma limit. Using Eq. (6) with $\epsilon^2 = 0$
and the fact that the WKB solutions vary as $\exp(i\int k_{\parallel} d\hat{z})$, gives the WKB
dispersion relation,

$$- \hat{z} \, k_{\parallel}^2 + i\alpha k_{\parallel} + (\hat{z}\beta_2^2 - \beta_1) = 0 \, , \tag{41}$$

where the derivative of $k_{\parallel}$ has been assumed negligible. From (41) we
obtain

$$k_{\parallel} \approx i(\alpha/2 + i\beta_0)/\hat{z} + \beta_2 \, , \tag{42}$$

where terms of order $1/\hat{z}^2$ have been ignored since $\hat{z}$ is assumed large.
Using (42) then gives

$$i\int k_{\parallel} \, d\hat{z} = -(\alpha-a)\ln\hat{z} + i\beta_2\hat{z} \, , \tag{43}$$

so that the WKB solutions are proportional to $(\hat{z})^{a-\alpha}\exp(i\beta_2\hat{z})$. For
$\alpha = 1$ this behavior is the same as obtained in (38) and (40) for B_2
and B_3.

The functions $B_j(0)$ (with $j = 1,2,3$) are singular at the origin
because of the singularity in the function $U(a,\alpha;2i\beta_2\hat{z})$. For $\alpha = 1$ the
function U diverges as $\ln\hat{z}$ as $\hat{z}$ approaches zero. Thus near the origin the
ϵ^2 expansion of (23) is not useful for evaluating B_j. However, the
behavior of the solutions B_j near the origin can be determined by
expressing them in terms of the solutions B_0 and A_j as discussed in
section VI.

V. Mode Conversion:

In this section we consider the case of an electrostatic wave propagating in the whistler band incident upon plasma resonance from inside the plasma. In the whistler band the phase velocity is in the same direction as the group velocity (i.e., the whistler is a forward wave) so that, in the model plasma, the incident whistler is a positive phase velocity wave approaching the origin along the negative real z-axis. Thus we look for a solution at negative values of z, i.e. $\arg(z) = \pi$ which contains a part corresponding to a long wavelength incident wave (i.e., propagating from left to right) together, perhaps, with a reflected wave. On the other side of plasma resonance (i.e., $\arg(z)=0$) the solution must be bounded at infinity and be consistent with energy transport away from the origin. Thus for $\arg z = 0$ the solution must contain left to right propagating waves only.

From the discussion in section IV, a candidate solution for the incident wave is B_3 since it is long wavelength and propagates left to right for $\arg z = \pi$. From Fig. 4 we see, however, that the argument range of B_3 does not contain $\arg z = 0$ so that we can not directly determine the properties of B_3 on the other side of plasma resonance. To evaluate B_3 for $\arg z = 0$ we must analytically continue B_3 into this argument regime. Refering to Fig. 2 we note that the cut integration plane is free from singularities in the regions between the contours defining the solutions B_3, B_2 and A_1. The solution B_3 can then be related to the solutions B_2 and A_1 by extending the contour for B_3 to infinity in sector 2 and applying Cauchy's Theorem. This procedure yields the expression

$$B_3 = B_2 - e^{-i2\pi a} \cdot A_1 \ , \qquad (44)$$

which analytically continues B_3 into the desired argument range since as
shown in Fig. 4 the argument ranges of B_2 and A_1 both contain $\arg(z) = 0$.
The factor $e^{-i2\pi a_-}$ in (44) occurs because part of the distorted contour
for B_3 (the dashed portion in Fig. 2) lies on the Riemann sheet for which
the phase of the term $(\sigma - \sigma_0)^{\alpha_-}$ in (17) is 2π less than it is on the
principal sheet in which the defining contour for A_1 lies. The fact that
the analytic continuation involves the short wave length mode represented
by A_1 means that mode conversion must occur. Thus the mathematical
procedure of analytic continuation corresponds to the physical process of
mode conversion.

B_3 analytically continues into a physically acceptable solution
because, for $\arg(z)=0$, (38) indicates that asymptotically $(|z| \to \infty, \arg(z)=0)$
B_2 corresponds to a left to right propagating wave, while, from Fig. 3, we
note that A_1 also corresponds to a left to right propagating wave at arg z
$= 0$. Thus both waves transport energy away from plasma resonance. We
find then that a left-to-right propagating, purely long wavelength mode
(represented by B_3) incident upon plasma resonance from inside the plasma
gives rise to both a long wave length transmitted wave (represented by B_2)
and a short wave length transmitted wave (represented by A_1). The
transmission coefficient for the cold wave is $e^{-i\pi a}$, or $ie^{-\pi\beta_0}$. The
reflection coefficient is zero, i.e., there is no reflected wave. These
results are the same as obtained by Baños, et. al. (1986), who considered
only the purely cold case represented by the reduced equation (i.e., (6)
with $\varepsilon^2 = 0$).

In obtaining the asymptotic expressions for B_3, B_2, and A_1 we have
assumed that the magnitude of the function arguments is large. While this
assumption is consistent with the model plasma for negative values of z,

it is not for positive values of $\hat{z}$ when considering the function B_2.
This is because the region $\hat{z} > 1$ corresponds to a fictitious negative
value of plasma density arising from the approximation, $1 - \omega_p^2/\omega^2 = z/L$,
in the model. Thus while the argument of the function A_1, $\zeta = 2\hat{z}^{3/2}/3\varepsilon$
can be assumed large for values of $\hat{z} < 1$ because $\varepsilon^2 \ll 1$, the argument of
the function B_2 can not. However, an appropriate expression for the
function B_2 can be obtained by assuming that the magnitude of the
coefficient a in the Kummer functions $U(a,\alpha;w)$ and $M(a,\alpha;w)$ is large in
comparison to α and the magnitude of the independent variable w. In terms of
physical parameters this requirement becomes,

$$|\hat{z}| \ll \beta_1/(\beta_2^2) = \Omega^2/\omega^2 . \tag{45}$$

Since, for waves propagating in the whistler band, $\omega < \Omega$ the requirement
(45) can be satisfied for values of $\hat{z}$ with $\hat{z}_0 < \hat{z} < 1$, where again $\hat{z}_0$ is
arbitrary but small and non zero. Then, for $\arg(\hat{z}) = 0$ and large $|a|$,
$U(a,1;w)$ and $M(a,1;w)$ have the asymptotic behavior (Slater, 1970)

$$e^{-w/2} U(a,1;w) \sim \Gamma(1-a)[\cos(\pi a)J_0(i\chi) - \sin(\pi a)Y_0(i\chi)] , \tag{46.a}$$

$$e^{-w/2} M(a,1;w) \sim J_0(i\chi) , \tag{46.b}$$

where J_0 and Y_0 are zero order Bessel functions of the first and second
kind, respectively, and $\chi = 2(2\beta_0\beta_2\hat{z})^{1/2}$. Using (46.a,b) in (36) we then
obtain

$$B_2(0) \sim i\pi[J_0(i\chi) + iY_0(i\chi)] = 2K_0(\chi) , \tag{47}$$

where K_0 is the modified Bessel function. From (47) we see that, for
$\arg(\hat{z}) = 0$, B_2 represents a decaying function for increasing $|\hat{z}|$.

Thus, a long wavelength whistler incident upon plasma resonance from
inside the plasma gives rise, beyond plasma resonance, to a short wavelength
Bohm-Gross mode propagating towards decreasing density and a decaying long
wavelength structure. No energy is reflected back into the plasma from

the plasma resonance layer.

VI. Electric Field Structure Near Plasma Resonance

Having established that a whistler wave incident upon plasma resonance converts, without reflection, into a short wavelength thermal mode, we now determine the structure of the electric field near plasma resonance arising from the mode conversion process. We then relate the amplitude of the field at the origin to the asymptotic amplitude of the incident whistler wave.

The structure of the electric field of the incident cold mode in the vicinity of plasma resonance can not be obtained from expressions such as (23) because the function $B_3(0)$ is singular at the origin. The structure can be found, however, by relating the solution B_3 to the solutions A_j and B_0 which are not singular at the origin. In addition, this relation gives an expression for B_3 valid for all values of $\arg(\hat{r})$ when the series expressions for the functions A_j are used.

The relation useful for evaluating the behavior of B_3 near the origin is established by deforming the contours which define the solutions B_3 and A_2. As shown in Fig. 5.a, B_3 can be related to B_1, A_3 and A_1 by extending the contour defining B_3 to infinity in sectors 1 and 2. This procedure is permitted because the integrand in (12), the general expression for the solutions, is analytic in the cut s-plane over the region of distortion. Then by Cauchy's theorem we obtain the relation

$$B_3 = B_1 - A_3 - e^{-i2\pi a_-} A_1 . \tag{48}$$

The factor $e^{-i2\pi a_-}$ multiplying A_1 arises because the argument of the term $(s - i\beta_2)^{\alpha_-}$ in (12) is 2π less than over the basic defining contour for A_1 shown in Fig. 2. Likewise, the contour defining A_2 can be pulled into the point $s = -i\beta_2$ to coincide with the contours for B_1 and the combination $e^{i2\pi a_+} [e^{i2\pi a_-} B_3 + B_0]$ as shown in Fig. 5.b, giving

$$A_2 = -B_1 + e^{i2\pi a_+} [e^{i2\pi a_-} B_3 + B_0] \ . \tag{49}$$

The relations (48) and (49) can then be combined to give

$$B_3(\hat{z}) = [e^{i2\pi\alpha} - 1]^{-1} \left(A_2 + e^{-i2\pi a_-} A_1 + A_3 - e^{i2\pi a_+} B_0 \right) . \tag{50}$$

The expression (50) for $B_3(\hat{z})$ is valid for all $\arg(\hat{z})$ when the series expressions (21) for A_j are used, so that (50) represents the analytic continuation of B_3 into all $\arg(\hat{z})$ values for the finite $\hat{z}$-plane.

Note from (50) that the term outside the braces diverges as α approaches integer values, so that it must be the case

$$\underset{\alpha \to 1}{\text{Lim}} \left(A_2 + e^{-i2\pi a_-} A_1 + A_3 - e^{i2\pi a_+} B_0 \right) = 0 \ . \tag{51}$$

Using L'Hopital's Rule to evaluate (50) we then obtain

$$B_3 = \frac{1}{2\pi i} \left([\partial_\alpha A_2 + \partial_\alpha(e^{-i2\pi a_-}A_1) + \partial_\alpha A_3 - \partial_\alpha(e^{i2\pi a_+}B_0)]\big|_{\alpha=1} \right) . \tag{52}$$

Note that to obtain (52) it is necessary to treat α, the coefficient of the first derivative term in (6), as a general parameter as was first pointed out by Rabenstein (1958) in his extension of the work by Wasow (1953).

The function proportional to the electric field, B_3' (where ' denotes derivative with respect to argument), is given by

$$B_3' = \frac{1}{2\pi i} \left(\partial_\alpha A_2' + \partial_\alpha(e^{-i2\pi a_-}A_1') + \partial_\alpha A_3' \right) , \tag{53}$$

where the term proportional to the derivative of B_0 has been ignored in (53) because it is smaller, by a factor of $\varepsilon^{2/3}$, than the terms proportional to the derivatives of the functions A_j . Assuming that $\sigma_0 = i\varepsilon^{2/3}\beta_2 \ll 1$, the $m = 0$ term of the series expansion (21) can be used to evaluate (53) to obtain B_3' in terms of familiar functions,

$$B_3' \approx \pi [Gi(-\eta) + iAi(-\eta)] \ . \tag{54}$$

The details of this calculation are given in Appendix II. In (54), $Gi(-\eta)$

denotes a solution of the inhomogeneous, or driven, Airy equation and $Ai(-\eta)$ is a solution to the homogeneous Airy equation (Antosiewicz, 1970). The asymptotic form of the functions in (54) are

$$Ai(-\eta) \sim \pi^{-1/2}\eta^{-1/4} \sin(\zeta + \pi/4) , \qquad (55.a)$$

and

$$Gi(-\eta) \sim \pi^{-1/2}\eta^{-1/4} \cos(\zeta + \pi/4) - \pi^{-1}\eta^{-1} , \qquad (55.b)$$

where $\zeta = 2\eta^{3/2}/3$. From (55.a,b) it is clear that the electric field structure of the mode converted wave consists of a short scale length wave propagating down the density gradient away from plasma resonance together with a field that falls off slowly as $1/\eta$.

The electric field amplitude at the origin can be related to the asymptotic whistler amplitude by obtaining an approximation to Eq. (6) valid near the origin for $\alpha = 1$. With $\alpha = 1$, (6) can be integrated once to obtain

$$\varepsilon^2\phi^{(3)} + \mathfrak{z}\phi^{(1)} = \int^{\mathfrak{z}} (\beta_1 - \mathfrak{z}\beta_2{}^2)\phi \, d\mathfrak{z} + C , \qquad (56)$$

where C is a constant of integration. Now consider the mode conversion solution B_3 which satisfies (56). Near the origin $B_3(0)$, which is the leading term in the ε^2 expansion of B_3, is singular for small $\mathfrak{z}$, diverging as $\ln(\mathfrak{z})$. For the purpose of estimating the relative magnitudes of the terms in (56) for small $\mathfrak{z}$, B_3 (and, thus ϕ) can be approximated by $\ln(\mathfrak{z})$.

Since $\phi^{(1)}$ is proportional to $\mathfrak{z}^{-1}$, $\mathfrak{z}\phi^{(1)}$ is of order unity, while $\varepsilon^2\phi^{(3)}$ is proportional to $\varepsilon^2/\mathfrak{z}^3$. The terms on the left hand side of (56) are then of order unity, or larger, for small $\mathfrak{z}$. On the other hand, the integral term on the right hand side of (56) approaches zero. Evaluating this term we find,

$$\int^{\mathfrak{z}} (\beta_1 - \beta_2{}^2 \, \mathfrak{z})\ln(\mathfrak{z})d\mathfrak{z} = \beta_1(\mathfrak{z}\ln(\mathfrak{z})-\mathfrak{z}) -\beta_2{}^2(\mathfrak{z}^2\ln(\mathfrak{z})-\mathfrak{z}^2/2)/2 . \qquad (57)$$

Since $\mathfrak{z}\ln(\mathfrak{z})$ and $\mathfrak{z}$ are continuous and have the limit zero as $\mathfrak{z}$ goes to zero, the integral term on the right hand side of (56) can be made as

small as desired by chosing $\hat{z}$ small enough. Thus for $\hat{z} < \hat{z}_0$ where $\hat{z}_0$ is such that

$$\beta_1 \hat{z}_0(\ln(\hat{z}_0)-1) - \beta_2^2[\hat{z}_0^2(\ln(\hat{z}_0)-1/2)]/2 \ll \text{Min}(C,1) , \tag{58}$$

(56) can be approximated by

$$\varepsilon^2 \phi^{(3)} + \hat{z}\phi^{(1)} = C . \tag{59}$$

By setting $\phi^{(1)} = E$, the z-component of the electric field, and using $z = \hat{z}L$, (59) can be written in the form

$$\frac{\gamma \bar{v}^2}{\omega_{pe}^2} \frac{d^2}{dz^2} E + \frac{z}{L} E = E_0 . \tag{60}$$

Equation (60) describes plasma resonance driven by a constant electric field of amplitude E_0. Thus we interpret the constant C in (59) as an effective external electric field strength at the origin, E_0, which excites the Bohm-Gross mode. The solution to (59) is then

$$\phi^{(1)} = -\pi E_0 \varepsilon^{-2/3} [\text{Gi}(-\eta) + i\text{Ai}(-\eta)] . \tag{61}$$

Interpreting $\phi^{(1)}$ as an approximation to the solution B_3', i.e., $\phi^{(1)} = \bar{C} \partial_{\hat{z}} B_3$ where $\bar{C}$ is a constant of proportionality, we obtain

$$\bar{C} \partial_{\hat{z}} B_3 = -\pi \varepsilon^{-2/3} E_0 [\text{Gi}(-\eta) + i\text{Ai}(-\eta)] . \tag{62}$$

However, from (54) we have for small $\hat{z}$ (i.e., $\hat{z} < \hat{z}_0$)

$$\partial_\eta B_3 = \varepsilon^{2/3} \partial_{\hat{z}} B_3 = \pi[\text{Gi}(-\eta) + i\text{Ai}(-\eta)] , \tag{63}$$

from which we conclude that the proper choice of the constant $\bar{C}$ is $-E_0$ and

$$\phi^{(1)} = -E_0 \partial_{\hat{z}} B_3 . \tag{64}$$

Having used the behavior of B_3 near the origin to find the constant of proportionality between B_3' and $\phi^{(1)}$, we can now relate the field strength E_0 to the amplitude of the incident whistler wave. Since the electric potential of the incident whistler wave is represented, in the mode conversion solution, by B_3 for $|\hat{z}| \to \infty$, $\arg(\hat{z})=\pi$, we use the asymptotic form

of B_3 and (64) to make this connection. Asymptotically $\partial_{\bar{z}} B_3 \sim \partial_{\bar{z}} B_3(0)$ and from (40)

$$\partial_{\bar{z}} B_3(0) \sim i\beta_2 \, \Gamma(1\text{-}a) \, e^{i\pi a} \, w^{-(1\text{-}a)} e^{w/2} \, , \qquad (65)$$

so that

$$-E_0 \, \partial_{\bar{z}} B_3 \sim \beta_2 \, \Gamma(1/2+i\beta_0) \, e^{\pi\beta_0} \, E_0 \, w^{-(1\text{-}a)} e^{w/2} \, . \qquad (66)$$

Since, as discussed in Sec. IV, $w^{-(1\text{-}a)} \exp(w/2)$ represents the functional form of the asymptotic whistler, the coefficient of this term on the right hand side of (66) can be equated to the electric field amplitude of the whistler wave, which we denote as $\beta_2 E_W$. Using $|\Gamma(1/2+i\beta_0)|^2 = \sqrt{\pi}/\cosh(\pi\beta_0)$, we then obtain

$$|E_0| = \frac{e^{-\pi\beta_0} \, [\cosh(\pi\beta_0)]^{1/2}}{\sqrt{\pi}} \, E_W \, . \qquad (67)$$

Eq. (67) relates the asymptotic value of the whistler electric field to the value of the driver electric field of Eq. (60). In terms of physical quantities the parameter β_0 has the form

$$\beta_0 = \frac{\Omega^2}{2\omega(\Omega^2-\omega^2)^{1/2}} \, k_\perp L \, . \qquad (68)$$

VII. Conclusions

This analytic study has identified a new mode conversion process that can occur in magnetized plasmas having a longitudinal density gradient (i.e., $\nabla n_0 \times \vec{B} = 0$), as may apply in the auroral ionosphere and long mirror machines. It is demonstrated that an electrostatic whistler mode with frequency ω less than the electron gyrofrequency (i.e., $\omega < \Omega$) transfers all of its energy to a hot Bohm-Gross mode at that point in the density profile where $\omega = \omega_{pe}$. The excited hot plasma mode propagates away from plasma resonance in the direction of decreasing density and eventually transfers its energy to background electrons. Thus the mechanism described here provides a conceptual link between the presence of large amplitude whistler wave activity and the generation of magnetic field aligned fast electrons. Although no effort is devoted in the present study to an evaluation of the quantitative consequences expected for specific physical situations, this is a worthwhile project that requires a separate survey.

Our major effort has aimed at providing an analytical description of the mode conversion process and an evaluation of the structure of the electric field excited at plasma resonance. The solutions of the differential equation describing the mode conversion process are divided into two categories. One category of solutions has short wavelengths and is related to Bohm-Gross waves. These solutions do not exist in the cold plasma limit. Expressions useful for evaluating the asymptotic properties of these solutions are given in (20.a,b) while the series expression given in (21) is useful for evaluating the solutions near the origin. The second category of solutions is characterized by long wavelengths and includes solutions that

asymptotically represent propagating electrostatic whistler waves. The analytic expressions given in (29) and (36) in terms of Kummer functions are useful for evaluating these solutions away from the origin. The long wavelength solutions are evaluated near the origin by relating them to the series expressions of the short wavelength solutions. The physical process of mode conversion is shown to correspond to the mathematical procedure of analytic continuation which relates a long wavelength solution defined over a given argument range to a combination of short and long wavelength solutions defined over a separate argument range.

Although the details of the analysis presented are somewhat involved, they point to a powerful simplification in describing the mode conversion process. It is shown rigorously that at plasma resonance the excitation of the Bohm-Gross mode results as if it were driven by a uniform capacitor plate electric field, E_0, as has been invoked previously in other resonant excitation problems (Morales and Lee, 1974 ; Shoucri and Kuehl, 1980). The analytic expression given in Eq. (67) relates the effective pump field E_0 to the asymptotic whistler amplitude E_W, providing the connection needed to apply the capacitor plate model to an incident wave problem. The plasma properties appear through the single parameter $\beta_0 = k_\perp L\Omega^2/[2\omega(\Omega^2-\omega^2)^{1/2}]$.

Finally, we note that the analysis presented here complements and extends a previous study (Maggs, et.al., 1984) devoted to the properties of resonant excitation of a plasma driven externally at frequencies larger than the electron gyrofrequency (i.e., $\omega > \Omega$).

ACKNOWLEDGEMENTS

REFERENCES

Antosiewicz, H.A., Bessel Functions of Fractional Order, in Handbook of
Mathematical Functions, edited by M. Abramowitz and I.A. Stegun
pp. 435-478, Dover, New York, 1970.

Baños, A. Jr., J.E. Maggs and G.J. Morales, Anomalous Reflection
Exhibited by a Generalized Resonance-Tunneling Equation,
Phys. Rev. Letters, 56, 2433-2436, 1986.

Coddington, E.A. and N. Levinson, Theory of Ordinary Differential
Equations, Sec. 5.8, McGraw-Hill, New York, 1955.

Erdélyi, A., W. Magnus, F. Oberhettinger, and F. Tricomi, Higher
Trancendental Functions, Bateman Manuscript Project, Vol. 1,
McGraw-Hill, New York, 1953.

Maggs, J.E., A. Baños Jr. and G.J. Morales, Solutions of a Fourth
Order Differential Equation Describing Mode Conversion in a
Magnetized Plasma, J. Math. Phys., 25, 1605-1618, 1984.

Morales, G. J. and Y.C. Lee, Ponderomotive-force Effects in a Non-uniform
Plasma, Phys. Rev. Lett., 33, 1016, 1974.

Rabenstein, A.L., Asymptotic Solutions of $u^{iv} + \lambda^2(zu''+\alpha u'+\beta u)=0$
for Large $|\lambda|$, Arch. Rat. Mech. Anal., 1, 408, 1958.

Shoucri, M., and H.H. Kuehl, 'Nonlinear Effects on the Mode Conversion of
Upper Hybrid Waves', Physics of Fluids, 23, 2461-2471, 1980.

Slater, L.J., Confluent Hypergeometric Functions, in Handbook of
Mathematical Functions, edited by M. Abramowitz and I.A. Stegun
pp. 504-535, Dover, New York, 1970.

Wasow, W., Asymptotic Solution of the Differential Equation Governing
Hydrodynamic Stability in a Domain Containing a Transition Point,
Ann. Math., 58, 222, 1953.

Appendix I:

In this appendix a series representation of the solutions A_j is derived by expanding the integrand of (17) in a series in σ_0/σ and integrating term by term. Writing

$$(\sigma-\sigma_0)^{\alpha_-}(\sigma+\sigma_0)^{\alpha_+} = \sigma^{\alpha-2} \sum_{m=0}^{\infty} c_m \, (\sigma_0/\sigma)^m \ , \qquad (I.1)$$

where the coefficients c_m are

$$c_m = \sum_{n=0}^{\infty} (-)^n \binom{\alpha_-}{n} \binom{\alpha_+}{m-n} \ , \qquad (I.2)$$

and $\binom{\alpha}{n} = \dfrac{\alpha!}{n!(\alpha-n)!}$ is the familiar binomial coefficient, gives

$$A_j = p_j \, \varepsilon^{-2(\alpha-1)/3} \sum_m c_m \, \sigma_0^m \, g(\eta,\alpha-m) \ , \qquad (I.3)$$

where

$$g(\eta,\alpha-m) = \int_{C(A_j)} d\sigma \, \sigma^{\alpha-m-2} \exp\left(-(\sigma^3/3 + \sigma\eta) \right) \ . \qquad (I.4)$$

The factors p_j in (I.3) are the same as defined for the asymptotic representation of the functions A_j given in (20.a,b). Expanding $\exp(-\sigma\eta)$ in a series then gives

$$g(\eta,\alpha) = \sum_k \frac{(-)^k}{k!} \, I(\alpha,k) \ , \qquad (I.5)$$

where the functions $g(\eta,\alpha)$ are the same as used by Rabenstein (1958), and

$$I(\alpha,k) = \int_{C(A_j)} d\sigma \, \sigma^{\alpha-2-k} \exp\,(-\sigma^3/3) \ . \qquad (I.6)$$

The integral in (I.6) can be evaluated by making the change of variable, $y = \sigma^3/3$. The contour corresponding to A_j then transforms into one which starts at infinity with argument $2\pi + 2\pi(2-j)$, encircles the origin in the counter-clockwise direction, and ends at infinity with argument $4\pi + 2\pi(2-j)$. Such contours correspond to Hankel's contour (Erdélyi, et.al., 1953) so that (I.6) can be written in the form,

$$I_j(\alpha,k) = 2\pi i \, \exp\left[\pi i(1-\rho)(7-2j)\right] \, / \, \left(3^\rho \, \Gamma(\rho)\right) , \qquad (I.7)$$

where $\rho = (4-\alpha-k)/3$. Using (I.7), (I.5) and (I.3) then gives a series expression for A_j valid in the finite z-plane for all values of $\arg(z)$,

$$A_j = \varepsilon^{-2(\alpha-1)/3} P_j \sum_k \sum_m c_m \, \sigma_0^{\,m} \frac{(-)^k}{k!} \, I_j(\alpha-m,k) \, \eta^k . \qquad (I.8)$$

Appendix II

In this appendix the functional form of the electric field of the mode conversion solution B_3' is obtained in terms of the Airy function, Ai, and the driven-Airy function, Gi. Starting with equation (53) which gives B_3' in terms of the derivatives of the functions A_j' with respect to α, namely,

$$B_3' = \frac{1}{2\pi i} \left(\partial_\alpha A_2' + \partial_\alpha(e^{-i2\pi a} A_1') + \partial_\alpha A_3' \right) , \qquad (II.1)$$

and using the m=0 term of the series representation of the functions A_j given by Eq. (21) or (I.8), we obtain

$$\partial_\alpha A_j' = [\partial_\alpha \ln p_j - \frac{2}{3} \ln \epsilon] A_j' + p_j \sum_{k=1}^{\infty} \frac{(-)^k}{(k-1)!} \partial_\alpha I_j \, \eta^{k-1} , \quad (II.2)$$

where

$$\partial_\alpha I_j = \frac{1}{3} [\pi i(7-2j) + \ln 3 + \psi(\rho)] I_j , \qquad (II.3)$$

with $\psi(\rho) = d[\ln \Gamma(\rho)]/d\rho$ and where I_j is given by (22) or (I.7). Defining the coefficients

$$C_j = \frac{p_j}{3} \sum_{k=1}^{\infty} \frac{(-)^k}{(k-1)!} \psi(\rho) I_j(\rho) \, \eta^{k-1} , \qquad (II.4)$$

we can then obtain from (II.1) using (51) and (II.2)

$$B_3' = [2e^{-i2\pi a} A_1' + A_3']/3 + [C_2 + e^{-i2\pi a} C_1 + C_3] . \qquad (II.5)$$

Since I_j is inversely proportional to $\Gamma(\rho)$, where $\rho = (3-k)/3$ when $\alpha=1$, the factors C_j contain the term

$$T = \psi(\rho)/\Gamma(\rho) = \Gamma'(\rho)/\Gamma^2(\rho) . \qquad (II.6)$$

To evaluate this term it is convenient to split the sum over k into three separate sums where

in case 1: $\qquad k = 3\ell \; ; \quad \ell = 0,1,2,\ldots \quad$, $\qquad (II.7.a)$

in case 2: $\qquad k = 3n + 1 \; ; \quad n = 1,2,3,\ldots \quad$, $\qquad (II.7.b)$

and in case 3: $k = 3m + 2$; $m = 1, 2, 3, \ldots$ (II.7.c)

Using the various values of k in (II.7) then gives for

case 1: $\rho = \ell - 1$; $T = (-)^{\ell}(\ell - 1)!$, (II.8)

case 2: $\rho = 2/3 - n$; $T = (-)^n \left(\frac{1}{3}\right)_n [\psi(2/3) + {}^n\left(\frac{1}{3}\right)]/\Gamma(2/3)$, (II.9)

where $\left(a \right)_n = \Gamma(a+n)/\Gamma(a)$, (II.10.a)

is Pochammer's symbol and we have defined a new symbol,

$${}^n\left(a \right) \equiv \sum_{j=0}^{n-1} \frac{1}{j+a} \quad , \tag{II.10.b}$$

and, case 3:

$$\rho = 1/3 - m \; ; \; T = (-)^m \left(\frac{2}{3}\right)_m [\psi(1/3) + {}^m\left(\frac{2}{3}\right)]/\Gamma(1/3) \; . \tag{II.11}$$

The calculation of B_3' is further facilitated by employing the following

notation

$$f(z) = \sum_{n=0}^{\infty} \frac{3^n}{(3n)!} \left(\frac{1}{3}\right)_n z^{3n} = \sum_{n=0}^{\infty} f_n \; ; \; fi(z) = \sum_{n=0}^{\infty} {}^n\left(\frac{1}{3}\right) f_n \; , \tag{II.12}$$

$$g(z) = \sum_{m=0}^{\infty} \frac{3^m}{(3m+1)!} \left(\frac{2}{3}\right)_m z^{3m+1} = \sum_{m=0}^{\infty} g_m \; ; \; gi(z) = \sum_{m=0}^{\infty} {}^m\left(\frac{2}{3}\right) g_m \; , \tag{II.13}$$

and $$h(z) = \sum_{l=1}^{\infty} \frac{3^{(\ell-1)}}{(3\ell-1)!} (\ell-1)! \; z^{3\ell-1} \; . \tag{II.14}$$

Using the series notation given in (II.12-14) and splitting the sum over

k into sums over ℓ, m, and n, the factors C_j can be written as

$$C_j = 2\pi i \; p_j \; e^{\pi i(7-2j)/3} \left\{ \frac{1}{3} h(\bar{\eta}) - c_1 [\psi(2/3)f(\bar{\eta}) + fi(\bar{\eta})] \right.$$
$$\left. + c_2 [\psi(1/3)g(\bar{\eta}) + gi(\bar{\eta})] \right\} \; , \tag{II.15}$$

where

$$c_1 = 1/[3^{2/3}\Gamma(2/3)] \; ; \; c_2 = 1/[3^{1/3}\Gamma(1/3)] \; ; \; \bar{\eta} = e^{\pi i(7-2j)/3} \eta \; . \tag{II.16}$$

Using (II.15) together with the relation,

$$A_j' = 2\pi i \; p_j \; e^{\pi i(7-2j)/3} \left(c_2 \; g(\bar{\eta}) - c_1 \; f(\bar{\eta}) \right) \; , \tag{II.17}$$

which can be obtained from the series representation of A_j by splitting

the sum over k into separate sums over ℓ,m,n and noting $\Gamma^{-1}(-\ell) = 0$,

B_3' can be written from (II.5) as

$$B_3' = f(-\eta)\left[\ \frac{2\pi i}{3}\ c_1\ (2e^{-\pi i/3} + e^{\pi i/3}) + \bar{c}c_1\psi(2/3)\right] + \bar{c}c_1 fi(-\eta)$$

$$-g(-\eta)\left[\ \frac{2\pi i}{3}\ c_2\ (2e^{\pi i/3} + e^{-\pi i/3}) + \bar{c}c_2\psi(1/3)\right] + \bar{c}c_2 fi(-\eta)$$

$$- h(-\eta)\ , \qquad\qquad\qquad (II.18)$$

where $\bar{c} = 1 + e^{2\pi i/3} + e^{-2\pi i/3}$. Noting that $\bar{c} = 0$, then gives

$$B_3' = \frac{2\pi i}{3}\left\{\ (1+e^{-i\pi/3})c_1 f(-\eta)\ -\ (1+e^{i\pi/3})c_2 g(-\eta)\right\} - h(-\eta)\ , \quad (II.19)$$

From the definition of the Airy functions (Antosiewicz, 1970)

$$Ai(x) = c_1 f(x) - c_2 g(x)\ , \qquad\qquad (II.20.a)$$

and $\qquad Gi(x) = 3^{-1/2}[c_1 f(x) + c_2 g(x)] + \pi^{-1}h(x)\ . \qquad\qquad (II.20.b)$

B_3' can be simply written using (II.19) and (II.20.a,b) as

$$B_3' = \pi[\ Gi(-\eta) + iAi(-\eta)]\ . \qquad\qquad (II.21)$$

FIGURES

Figure 1. An electrostatic whistler with frequency ω, less than the electron gyrofrequency Ω, propagates to plasma resonance (i.e., the point in the plasma where $\omega = \omega_{pe}$) located at $\tilde{z}=0$. The gradient in the plasma density is co-linear with the magnetic field.

Figure 2. The integration plane is cut by branch lines extending from the branch points $s = \pm i\beta_2$ to infinity parallel to the real axis. The contours defining the long wavelength solutions to (6) all start at the point $s = -i\beta_2$. Examples of the contours for this class of solutions which are related to the solutions of the reduced equation (8) are B_0, B_3, and B_2. The contours are shown as solid lines when they lie in the principal Riemann sheet and dashed lines when they lie in an adjacent sheet. The contour labeled A_1, which extends to infinity in sectors 2 and 3, is an example of a short wavelength solution.

Figure 3. The argument range of $\tilde{z}$ over which the asymptotic expressions for A_j given in (20.a) and (20.b) are valid are shown for each saddle point $\sigma = \pm i\eta^{1/2}$. The function behavior at values of $\arg(\tilde{z})$ integer multiples of $\pi/3$ is also indicated. Specifically, A_1 behaves asymptotically as a left to right propagating wave at $\arg(\tilde{z}) = 0$.

Figure 4. The principal argument ranges for the functions B_j ($j = 1,2,3$) are shown in relation to those for A_j . Asymptotically, the functions B_2

and B_3 represent left to right propagating, long wavelength waves at $\arg(\tilde{z}) = 0$ and π, respectively. The function B_1 asymptotically contains waves propagating in both directions for $\arg(\tilde{z}) = -\pi$. The argument range of the function B_0 is not restricted. At $\arg(\tilde{z}) = 0$, B_0 contains both left and right propagating waves.

Figure 5. a). The defining contour for the function B_3 can be distorted to coincide with the contours defining B_1, A_3 and A_1. Cauchy's Theorem can then be used to produce a relation among these solutions useful for analytically continuing B_3.

      b). A_2 can be related to B_1 and a combination of B_0 and B_3 by distorting the defining contour and applying Cauchy's Theorem. In addition to pulling the contour in towards the point $s = -i\beta_2$, the lower half of the contour for A_2 is pulled around the point $s = i\beta_2$ in the counter-clockwise direction and back towards $s = -i\beta_2$ after passing onto the adjacent Riemann sheet.
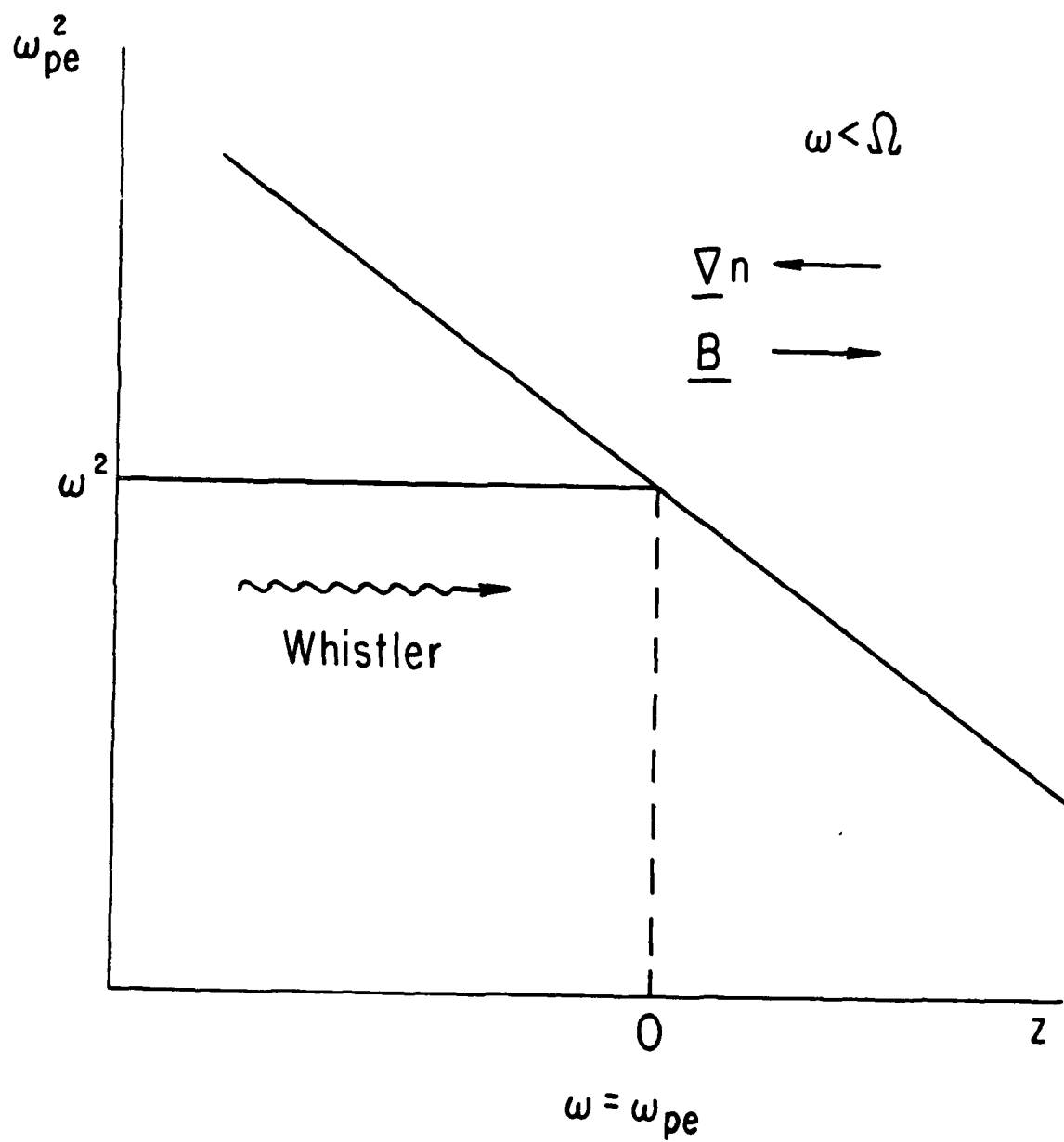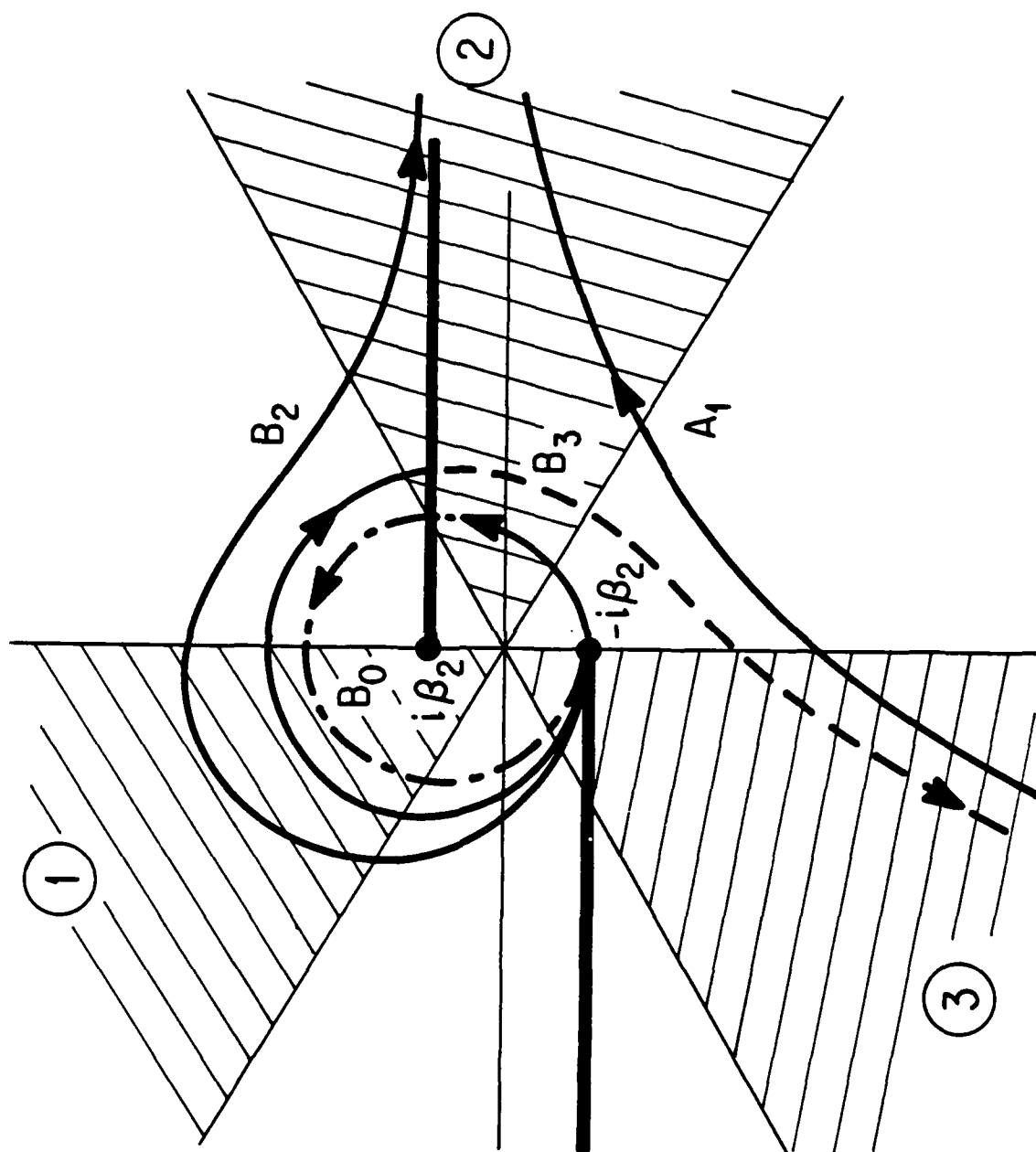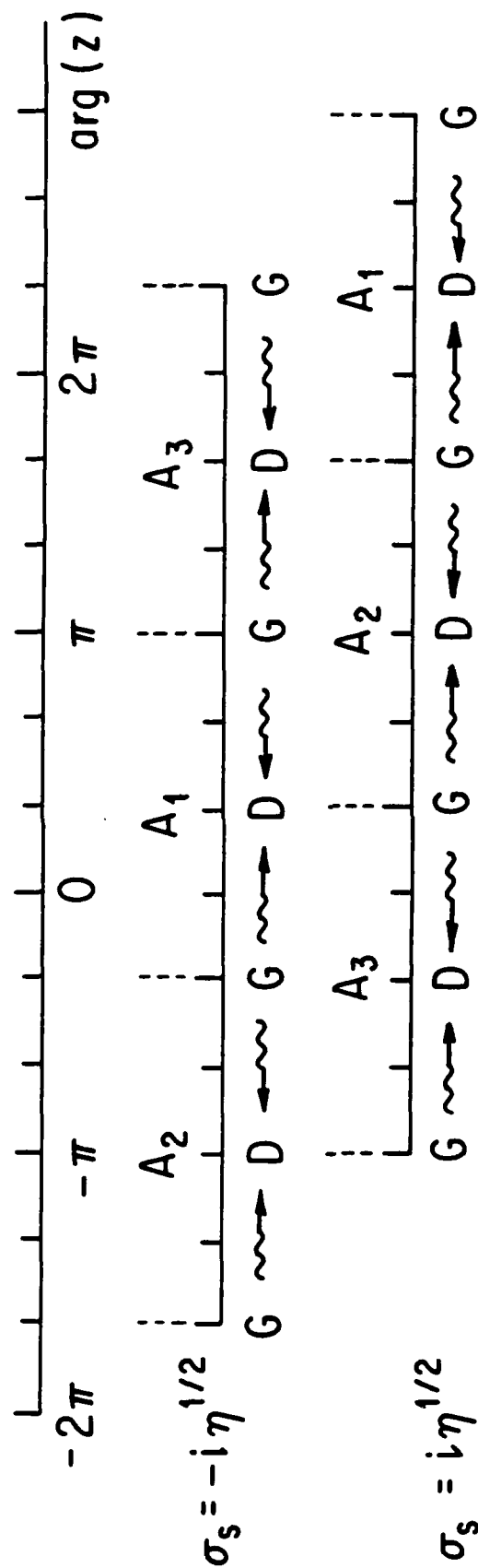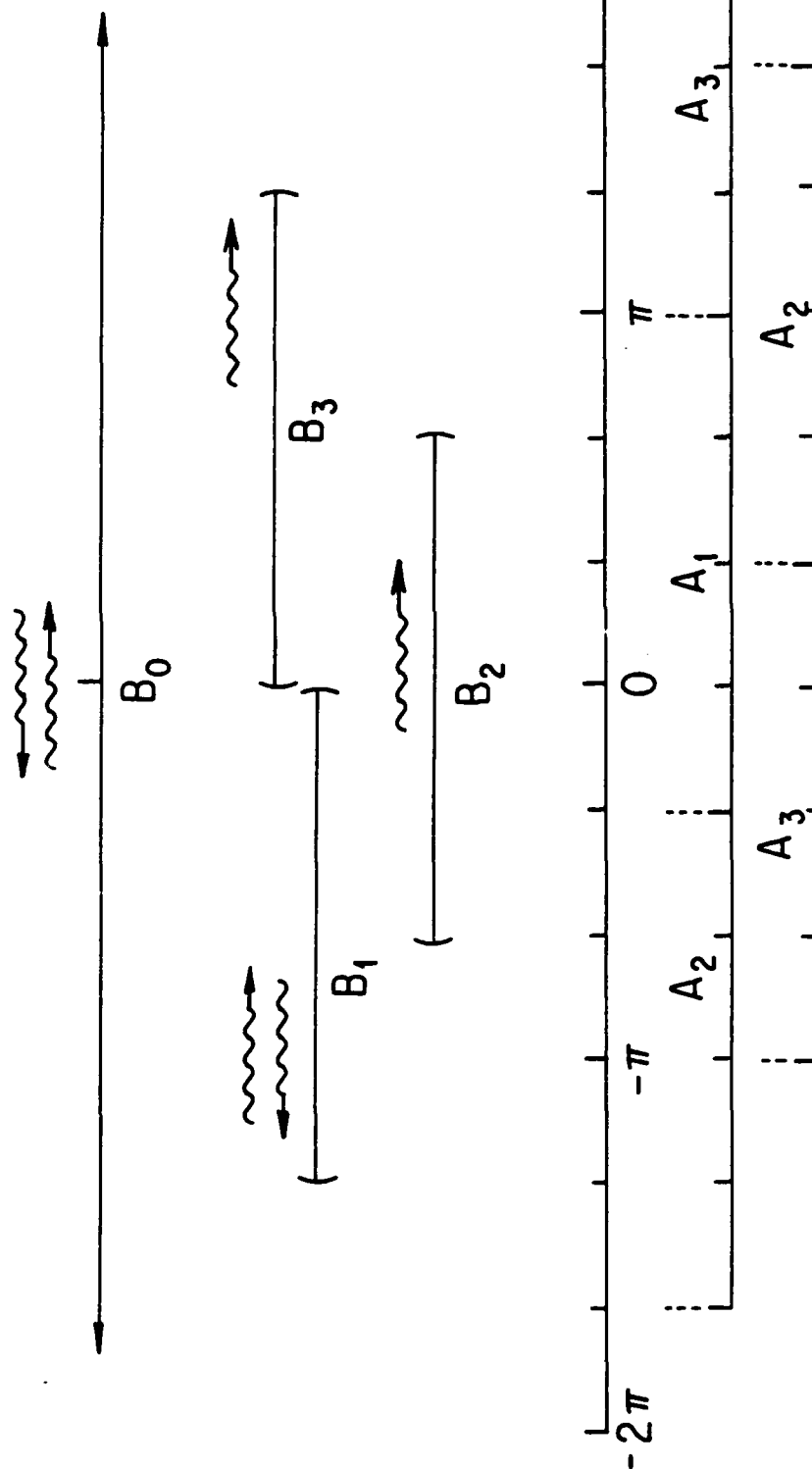
Figure 1

Figure 2
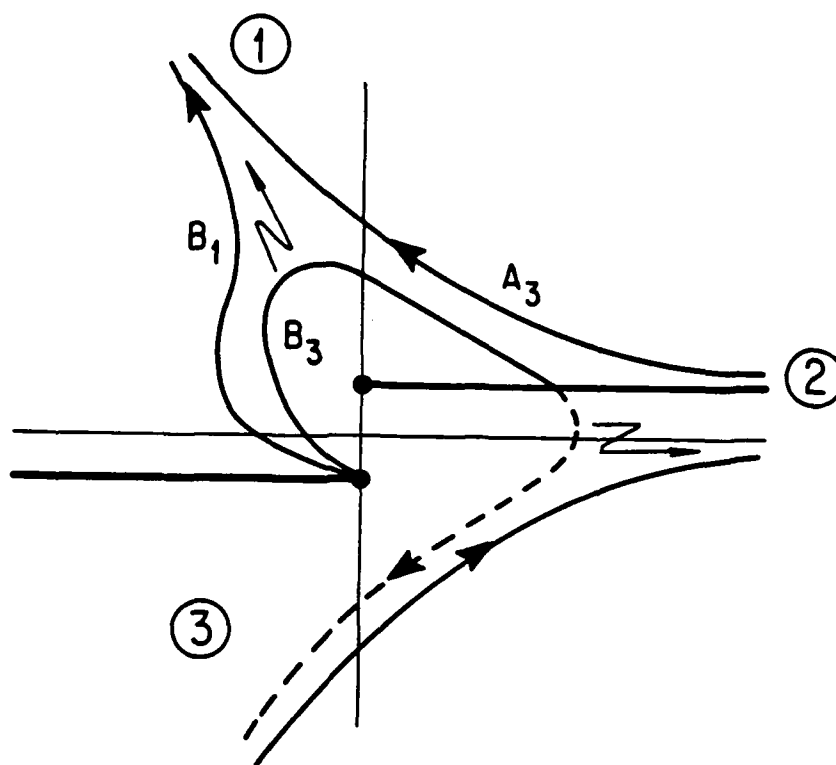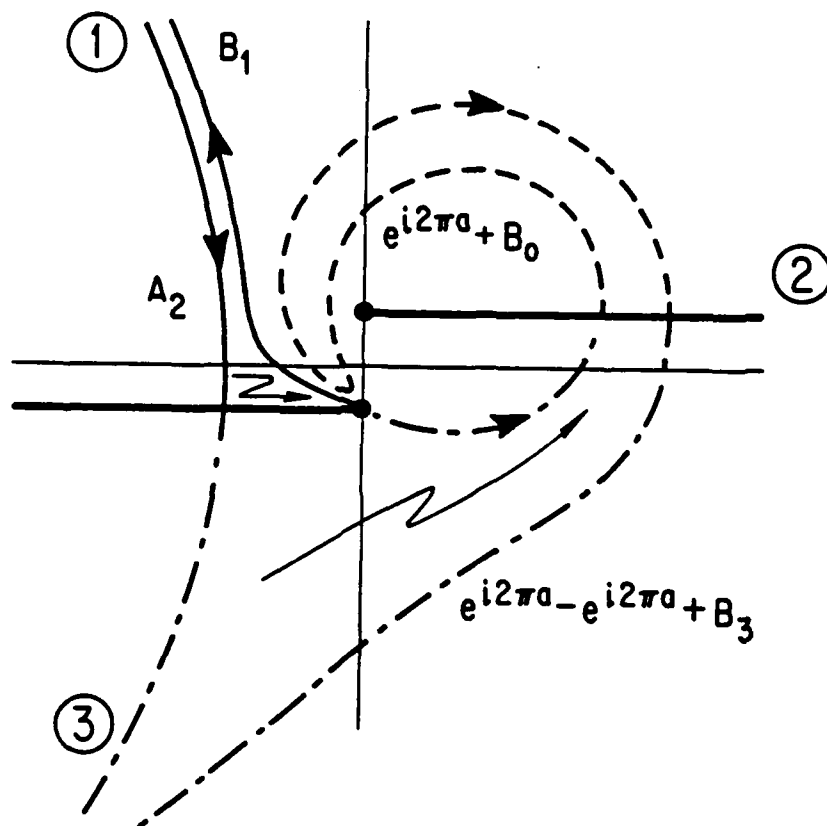
Figure 3

Figure 4

Figure 5

PPG-1106 "Nonlinear Resonance of Two-Dimensional Ion Layers", S.A. Prasad and G.J. Morales, submitted to The Physics of Fluids, September, 1987.

PPG-1107 "Laser Accelerators," Francis F. Chen, to be published in the Handbook of Plasma Physics, October, 1987.

PPG-1108 "Ion Bernstein Modes in Current-Carrying Plasmas," J. L. Milovich, Ph.D. dissertation, October, 1987.

PPG-1109 "Optimum Rankine Cycle for High Power Density Fusion Reactor Using Liquid Metal as Primary Coolant", M. Hasan, D. Sze, Report, January, 1988.

PPG-1110 "Titan Reverse-Field Pinch Fusion Reactor Study," F. Najmabadi, et al., present at IEEE 12th Symposium on Fusion Engineering, October 12-16, 1987, Monterey, Calif., October, 1987.

PPG-1111 "Revised Benchmark Timings with Particle Plasma Simulation Codes," V.K. Decyk, (revision of PPG-950), October 1987.

PPG-1112 "Gain and Bandwidth of the Gyro-TWT and Carm Amplifier," K.R. Chu and A.T. Lin, October 1987.

PPG-1113 "Detailed Experimental Observations of the Tearing of an Electron Current Sheet", Walter Gekelman and Hans Pfister, submitted to Physics of Fluids, October 1987.

PPG-1114 "Instability of the Sheath Plasma Resonance", R.L. Stenzel, submitted to Physics of Fluids, October 1987.

PPG-1115 "Experimental Study of Time-Varying Current Flow Between Electrodes Immersed in a Laboratory Magnetoplasma," J. Manuel Urrutia, Ph.D. Dissertation, October 1987.

PPG-1116 "Counterstreaming Electron-Beam Beat-Wave Accelerator," Y.T. Yan, C.J. McKinstrie, T. Katsouleas, and J.M. Dawson, accepted for publication in Phys. Review A (December 1987), October 1987.

PPG-1117 "The TITAN Reversed-field Pinch Fusion Reactor Study", R.W. Conn, F. Najmabadi, and the TITAN research group, submitted for Proc. of IEEE 12th Symposium on Fusion Engineering, Monterey, CA, Oct. 12-16, 1987, November 1987.

PPG-1118 "Comparative Study of Cross-Field and Field Aligned Electron Beams in Experiments," R.M.Winglee and P.L.Pritchett, submitted to Journal of Geophysical Research, November 1987.

PPG-1119 "Theory, Design, and Operation of High Harmonic Gyro-Amplifiers" David F. Furuno, Ph.d disseration, December 1987.

PPG-1120 "Fluid Theories of Slow Shock Structure", C.F. Kennel, December 1987.

PPG-1121 "Plasma Acceleration of Particle Beams," T. Katsouleas and J.M. Dawson, to appear in Physics of Particle Accelerators, Vol. V., 1988 (Jan. 1988).

PPG-1122 "Diamagnetic Drift Effects on Ion Bernstein Mode Propagation in a Plasma Slab," R. D. Ferraro and B. D. Fried, submitted to Phys. Fluids, January 1988.

PPG-1123 "Hydrogen Pumping and Release by Graphite Under High Flux Plasma Bombardment," Y. Hirooka, W.K. Leung, R.W. Conn, D.M. Goebel, B. Labombard, R. Nygren, K.L. Wilson submitted to Journal of Vaccum Science and Technology, January 1988.

PPG-1124 "1987 Research Highlights in The Pisces Program," R.W. Conn, et al, January 1988.

PPG-1125 "Magnetic Fusion Energy, vol. 5. Technical Assessement of Critical Issues in the Steady State Operation of Fusion Confinement Devices," D. M. Goebel, Assessment Chairman, et al, January 1988.

PPG-1126 "A Particle MHD Simulation Approach with Application to a Global Comet-Solar Wind Interaction Model," R. Sydora and J. Raeder, January 1988, sub. to Cometary and Solar Plasma Physics.

PPG-1127 "Particle Collector Scoops for Improved Exhaust In 'Axi-semetric' Devices," R.W. Conn and G.H. Wolf, November 1987, sub. to Fusion Eng. and Design (2/88).

PPG-1128 "Fusion Core Start-Up, Ignition and Burn Simulations of Reverse-Field Pinch (R.F.P.) Reactors," Yuh-Yi Chu, (Ph.D. Dissertation), 2/88.

PPG-1129 "Nonlinear, Dispersive, Elliptically Polarized Alfven Waves," C.F. Kennel, B. Buti, and R. Pellat, submitted to Phys. of Fluids, February 1988.

PPG-1130 "Heating Efficiency of Beat-Wave Excitation in a Density Gradient," G.J. Morales and J.E. Maggs, February 1988.

PPG-1131 "Electrostatic Whistler Mode Conversion at Plasma Resonance," J.E. Maggs and G.J. Morales, February 1988.

PPG-1132 "Shock Structure in Classical Magnetohydrodynamics", C.F. Kennel, sub. to JGR, February 1988.

PPG-1133 "Generation and Propagation of Kilometric Radiation in the Auroral Plasma Cavity, P.L. Pritchett and R.M. Winglee, sub. to JGR, February 1988.

END

DATE

FILMED

7-88

DTIC